minerals

MDPI

Article

Pre-Alpine Tectono-Stratigraphic Reconstruction of the Jurassic Tethys in the High-Pressure Internal Piedmont Zone (Stura di Viù Valley, Western Alps)

Marcello De Togni *, Marco Gattiglio, Stefano Ghignone and Andrea Festa

Dipartimento di Scienze della Terra, Università degli Studi di Torino, Via Valperga Caluso 35, 10125 Torino, Italy; marco.gattiglio@unito.it (M.G.); s.ghignone@unito.it (S.G.); andrea.festa@unito.it (A.F.)

* Correspondence: marcello.detogni@edu.unito.it

Abstract: We present a detailed description of the tectono-stratigraphic architecture of the eclogite-facies Internal Piedmont Zone (IPZ) metaophiolite, exposed in the Lanzo Valleys (Western Alps), which represents the remnant of the Jurassic Alpine Tethys. Seafloor spreading and mantle exhumation processes related to the Alpine Tethys evolution strongly conditioned the intra-oceanic depositional setting, which resulted in an articulated physiography and a heterogeneous stratigraphic succession above the exhumed serpentinized mantle. "Complete" and "reduced" successions were recognized, reflecting deposition in morphological or structural lows and highs, respectively. The "complete" succession consists of quartzite, followed by marble and calcschist. The "reduced" succession differs for the unconformable contact of the calcschist directly above mantle rocks, lacking quartzite and gray marble. The serpentinite at the base of this succession is intruded by metagabbro and characterized at its top by ophicalcite horizons. Mafic metabreccia grading to metasandstone mark the transition between the "complete" and "reduced" successions. The character of the reconstructed succession and basin floor physiography of the IPZ metaophiolite is well comparable with the Middle Jurassic–Late Cretaceous succession of both the Queyras Complex (External Piedmont Zone) and the Internal Ligurian Units (Northern Apennines) and with modern slow-spreading mid-ocean ridges.

Keywords: tectono-stratigraphy; Piedmont Zone; metaophiolite; Western Alps; Alpine Tethys

Citation: De Togni, M.; Gattiglio, M.; Ghignone, S.; Festa A. Pre-Alpine Tectono-Stratigraphic Reconstruction of the Jurassic Tethys in the High-Pressure Internal Piedmont Zone (Stura di Viù Valley, Western Alps). *Minerals* **2021**, *11*, 361. https://doi.org/10.3390/min11040361

Academic Editor: Silvana Martin

Received: 1 March 2021
Accepted: 26 March 2021
Published: 30 March 2021

1. Introduction

During the rifting stage and seafloor spreading evolution of oceanic basins, the ocean floor commonly results the object of a strong tectono-stratigraphic mobility in response to the development of different types of active tectonic structures at different scales, such as extensional detachment faults, fracture zones, and transfer and tear faults (see, e.g., in [1–7]). The temporal and spatial development of these tectonic structures strongly controls the morphology of the oceanic basin, forming structural highs and lows that, in turn, influence the syn-extensional deposition, resulting in strong vertical and lateral facies and thickness variations (see, e.g., [5,8–18] and refrs. therein). The exposure of mantle rocks on the seafloor is also associated with serpentinization and ophicarbonation processes [7,19–21], which may form primary weakness horizons within the oceanic mantle.

During convergence tectonics both the intra-oceanic tectonic structures (i.e., extensional detachment faults, fracture zones, and transfer and tear faults) and the heterogeneous stratigraphy with its internal rheological contrasts (see, e.g., in [5,7–16] and references therein), represent, among others, important inherited weakness zones along which tectonic deformation commonly localizes (see, e.g., in [17,18,21–30]). Therefore, the tectono-stratigraphic reconstruction of the pre-orogenic oceanic basin physiography is highly significant to better constrain and understand the evolution of orogenic belts.

In exhumed polyphasic and metamorphosed orogenic belts, such as the Western Alps, the reconstruction of the pre-orogenic physiography of the oceanic basin (i.e., the Jurassic Alpine Tethys) is strongly complicated by the overprinting of a multistage, intense deformation and metamorphic recrystallization that these belts experienced during a complete orogenic cycle of oceanic subduction, continental collision, and exhumation.

Throughout detailed geological mapping, systematic structural, and stratigraphic observations, this paper documents the internal structure and stratigraphy of the eclogite-facies metaophiolite units of the Stura di Viù Valley in the axial zone of the Western Alps (Figure 1). The restoration of the syn-orogenic and polyphasic tectonic deformation of this sector allows us to distinguish and reconstruct the main tectono-stratigraphic characters of the intra-oceanic (pre-orogenic) ophiolite succession of a sector of the Jurassic Alpine Tethys (Ligurian-Piedmont Oceanic Basin), characterized by a strongly heterogeneous fossil mantle–sediment interface and preserved unconformities within the metasedimentary succession.

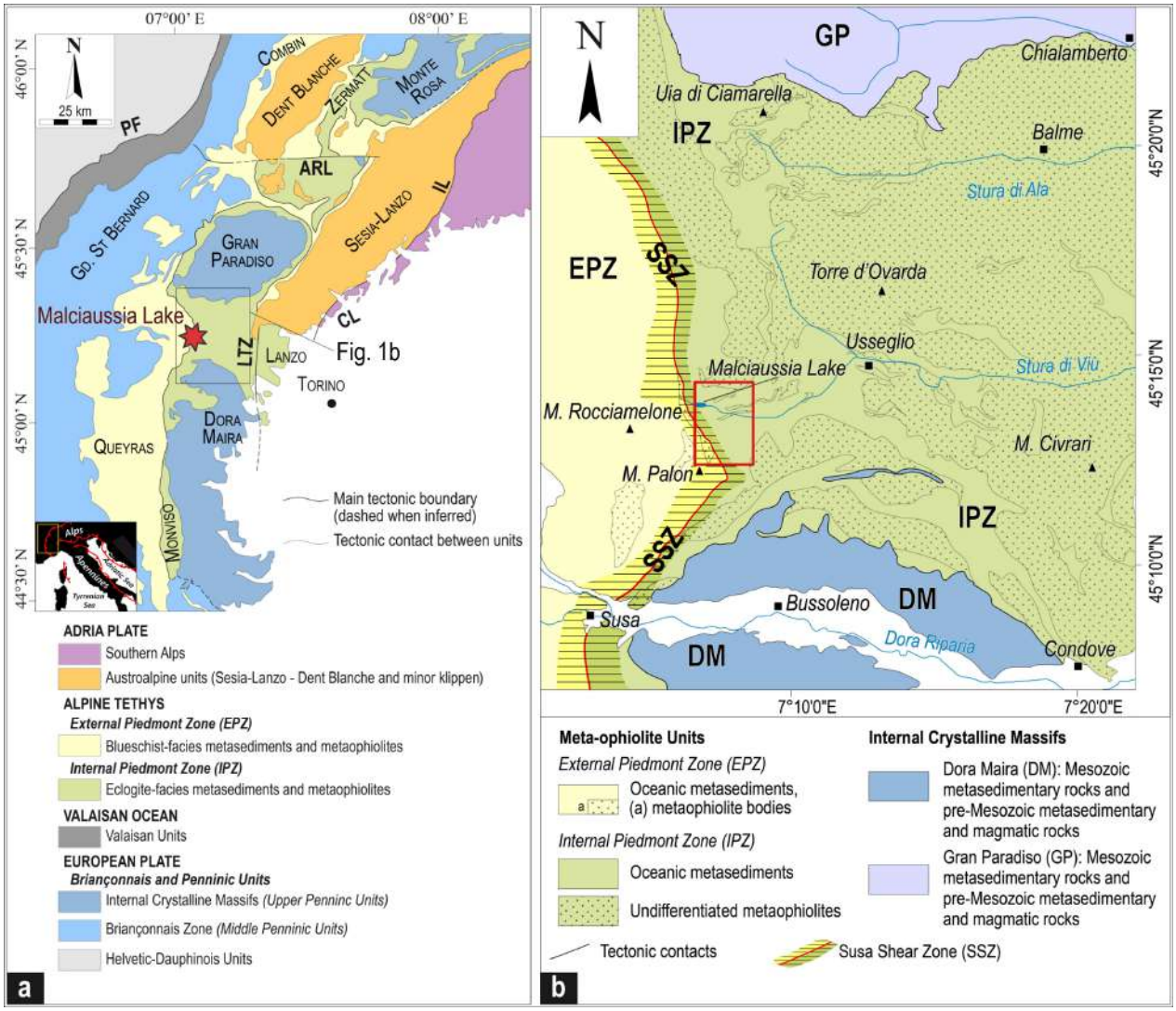

Figure 1. (**a**) Structural map of the Western Alps, modified after Balestro et al. [31]. ARL: Aosta-Ranzola fault, CL: Canavese Line, IL: Insubric Line, LTZ: Lis-Trana Fault Zone, PF: Penninic Front. Black square indicates the location of Figure 1b. (**b**) Structural sketch map of the Stura di Viù Valley area, modified after Nicolas [32], Perotto et al. [33], Bigi et al. [34], Ghignone et al. [35]. Red square indicates the study area.

2. Regional Geological Setting of the Western Alps

The Western Alps orogenic belt (Figure 1a) represents the result of complex geodynamic processes between the European and Adriatic continental margins and the interposed oceanic basin (i.e., the Alpine Tethys) [36–38]. The Alpine Tethys evolved after the Late Triassic–Early Jurassic rifting between these two continents, followed by the Middle to Late Jurassic seafloor spreading [17,39–42]. Subsequent alpine evolution mainly consisted of (I) subduction of the Tethyan oceanic lithosphere and distal European continental margin (Late Cretaceous to Middle Eocene), recording HP to UHP metamorphic conditions; (II) continental collision between the European and Adriatic margins (Late Eocene to Early Oligocene), resulting in the Alpine Tethys closure and exhumation of previously subducted oceanic and continental units; and (III) final deep Adriatic crust-mantle indentation and shallow crustal tectonics (Late Oligocene to Neogene) [17,42–49].

The axial sector of the Western Alpine belt represents an exhumed fossil subduction complex, corresponding to the most deformed (U)HP tectonometamorphic units [50,51], which consist of both ocean-derived and continental-derived rocks. The Western Alps metaophiolites (Piedmont Zone) represent the remnants of the Jurassic Alpine Tethys and are generally differentiated into (I) the eclogite-facies Internal Piedmont Zone (IPZ) and (II) the blueschist-facies External Piedmont Zone (EPZ), both tectonically overlying the thinned European continental palaeomargin (i.e., the Upper and Middle Penninic Units; see, e.g., in [52–54]).

The study area (Figure 1b) is located in the Stura di Viù Valley (Lanzo Valleys), which represents a sector of the Western Alps axial zone where the eclogite-facies metaophiolites of the IPZ are exposed. This area lacks detailed descriptions of the primary stratigraphic successions of metaophiolites and reconstruction of the pre-orogenic oceanic basin tectonostratigraphic setting. On the contrary, several studies documented its tectonometamorphic evolution [33,55–59]. This evolution resulted from four main alpine ductile deformational phases (D1–D4), which occurred under different metamorphic conditions and were closely related to those observed in the adjacent Susa Valley [35,58,60,61].

The IPZ likely reached the alpine eclogite metamorphic peak during early D1 deformation phase [56] for which different P-T peak conditions have been proposed, ranging from 13 kbar–450 °C to 29 kbar–530 °C [61–63]. The subsequent D2 deformation phase developed under greenschist facies metamorphic conditions during exhumation.

Later deformation phases (D3 and D4) document the alpine doming which involved the IPZ and the underlying Dora-Maira unit, forming a structurally homogeneous tectonic element [35,60]. Consequently, the western portion of the regional structural dome (i.e., Dora-Maira Unit and IPZ) suffered a regional-scale tilting with top-to-W extensional sense of shear, mostly developed along a first order shear zone separating the IPZ from the above EPZ [35,64,65]. This shear zone, that in the study area represents a polyphasic tectonic contact bounding the IPZ to both north and west (see Figure 2a), was recognized by various authors in the adjacent Susa Valley (i.e., the Susa Shear Zone of Ghignone et al. [35,65], Gasco et al. [66]) and in the northern Col de Entrelor (i.e., the Entrelor Shear Zone of Butler and Freeman [67], Malusà et al. [68]).

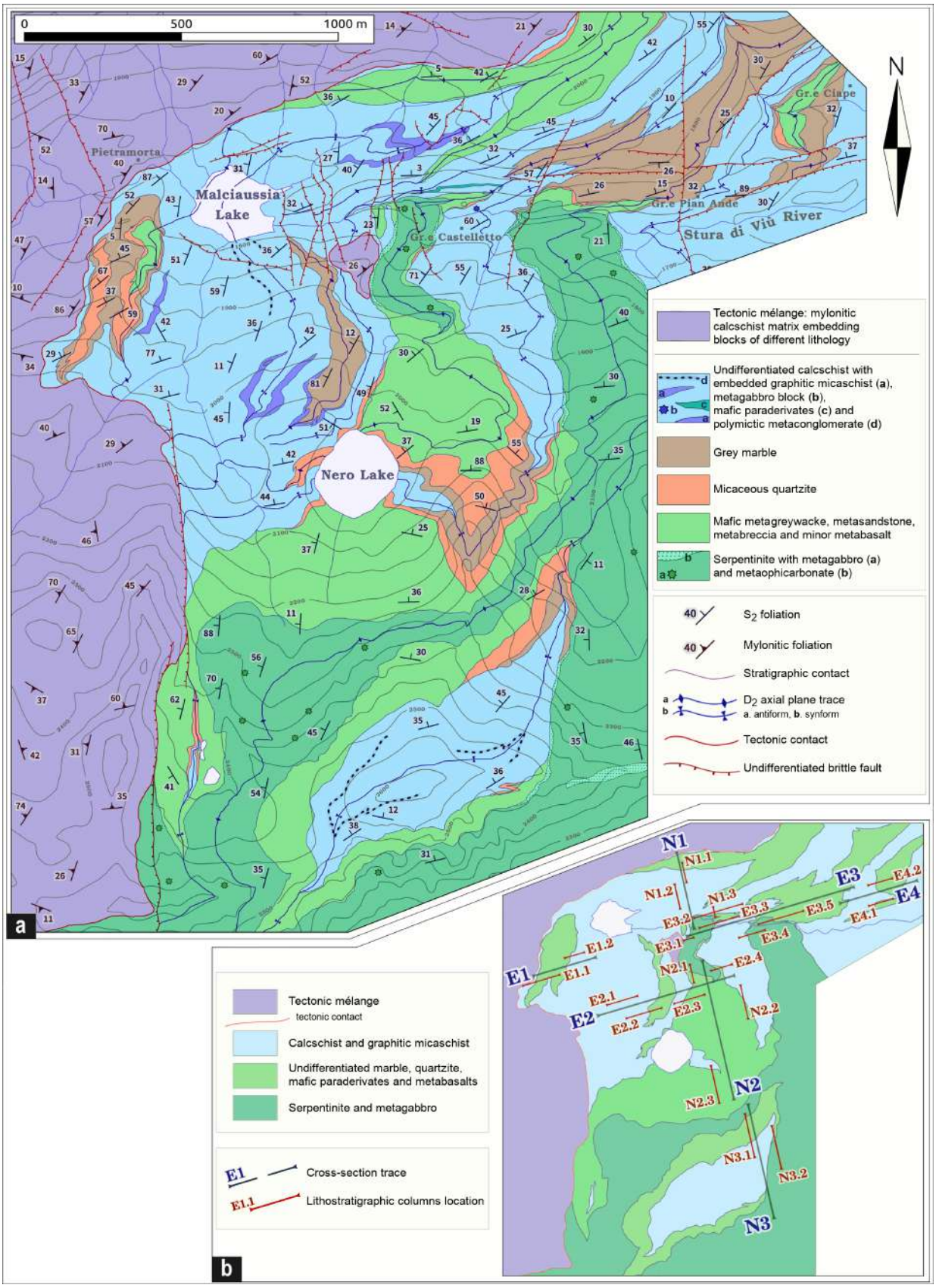

Figure 2. (**a**) Simplified geological map (1:10,000 scale) of the study area. (**b**) Schematic map showing the location of cross sections and lithostratigraphic columns. Schematic cross sections are shown in Figure 3. An integrated geological map showing the location of cross sections and lithostratigraphic columns is reported in Figure S1.

3. Methods

Geological and structural data, collected at 1:5000 scale during field mapping, are synthetized in a detailed geological map at 1:10,000 scale (Figure 2a). Four main regional deformational phases have been distinguished through overprinting and cross-cutting relationships among the different tectonic structures (see Section 5), such as the folds geometry and style, their interference patterns, the orientation of structural elements, and the sense of shear of kinematic indicators. The S2 foliation, which almost completely parallelizes the older S1 and S0 (i.e., primary stratigraphy) surfaces to D2 axial planes, has been recognized as the regional foliation and used as the reference surface (Figure 3).

Although pervasive tectonic overprinting was present, particular attention was dedicated to recognizing both primary stratigraphic contacts between different lithotypes and the remnants of the original stratigraphic succession (see Figures 4 and 5), whose details are shown through a dense grid of cross sections (*E1*, *E2*, *E3*, and *E4* and *N1*, *N2*, and *N3* in Figure 3), orthogonal to each other (i.e., E–W and N–S striking, respectively). Lithostratigraphic columns (*E1.1*, *E1.2*, *E2.1*, *N1.1*, *N1.2*, *N1.3*, etc.; see Figures 3, 6 and S1) have been realized where remnants of primary stratigraphic relationships among the different lithotypes have been recognized in order to reconstruct the characters of the stratigraphic succession.

Finally, optical microscope-based petrographic observations of the most significant lithotypes have been carried out in order to identify mineral assemblages and, mostly, to confirm field meso-scale evidences.

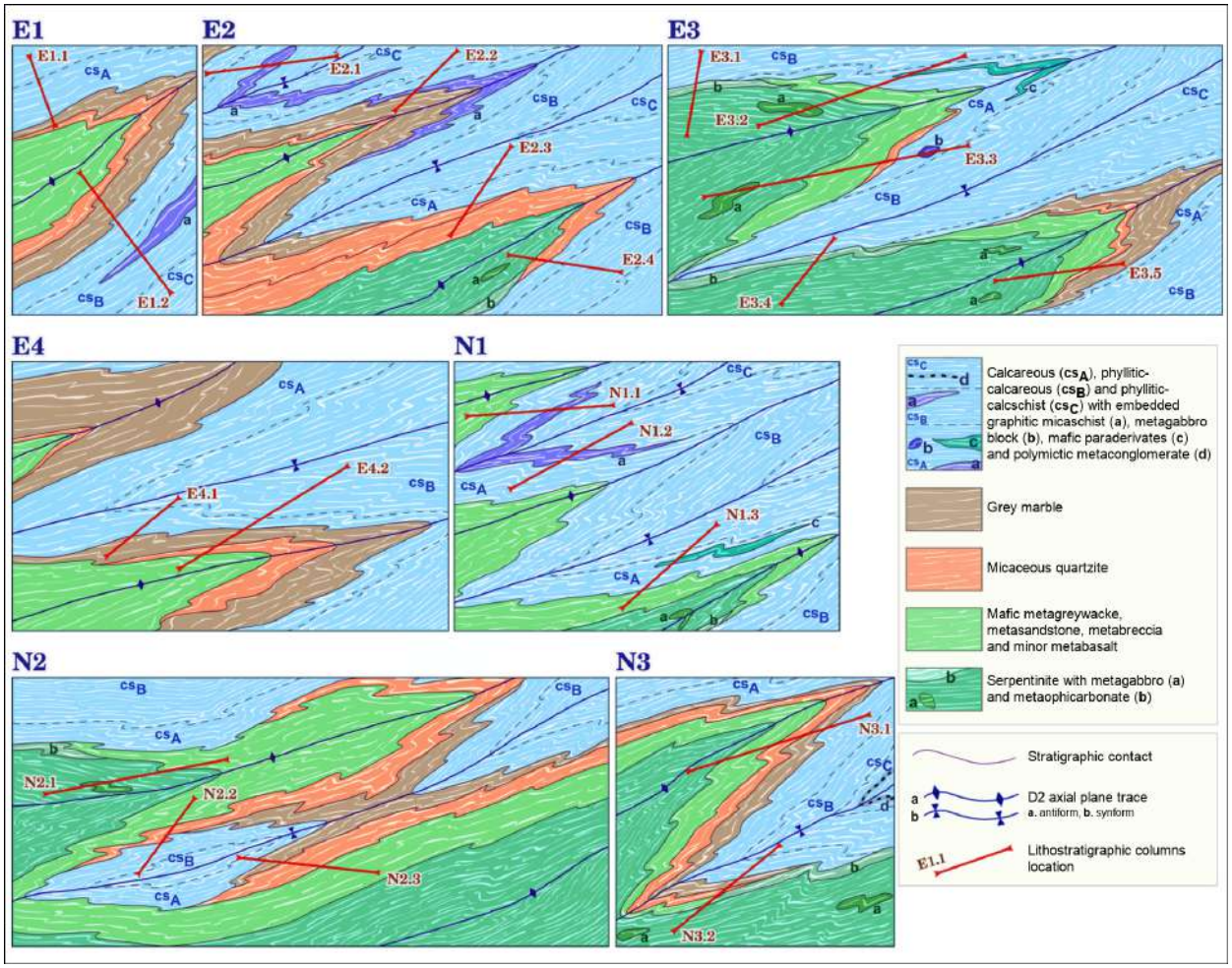

Figure 3. Schematic cross sections (not to scale) traced in Figure 2b, showing the geological-structural setting and related main deformational structures (i.e., D2 large-scale isoclinal sheath folds in *N2*). Red lines indicate the location of well-preserved stratigraphic sequences used for the reconstruction of lithostratigraphic columns shown in Figure 6.

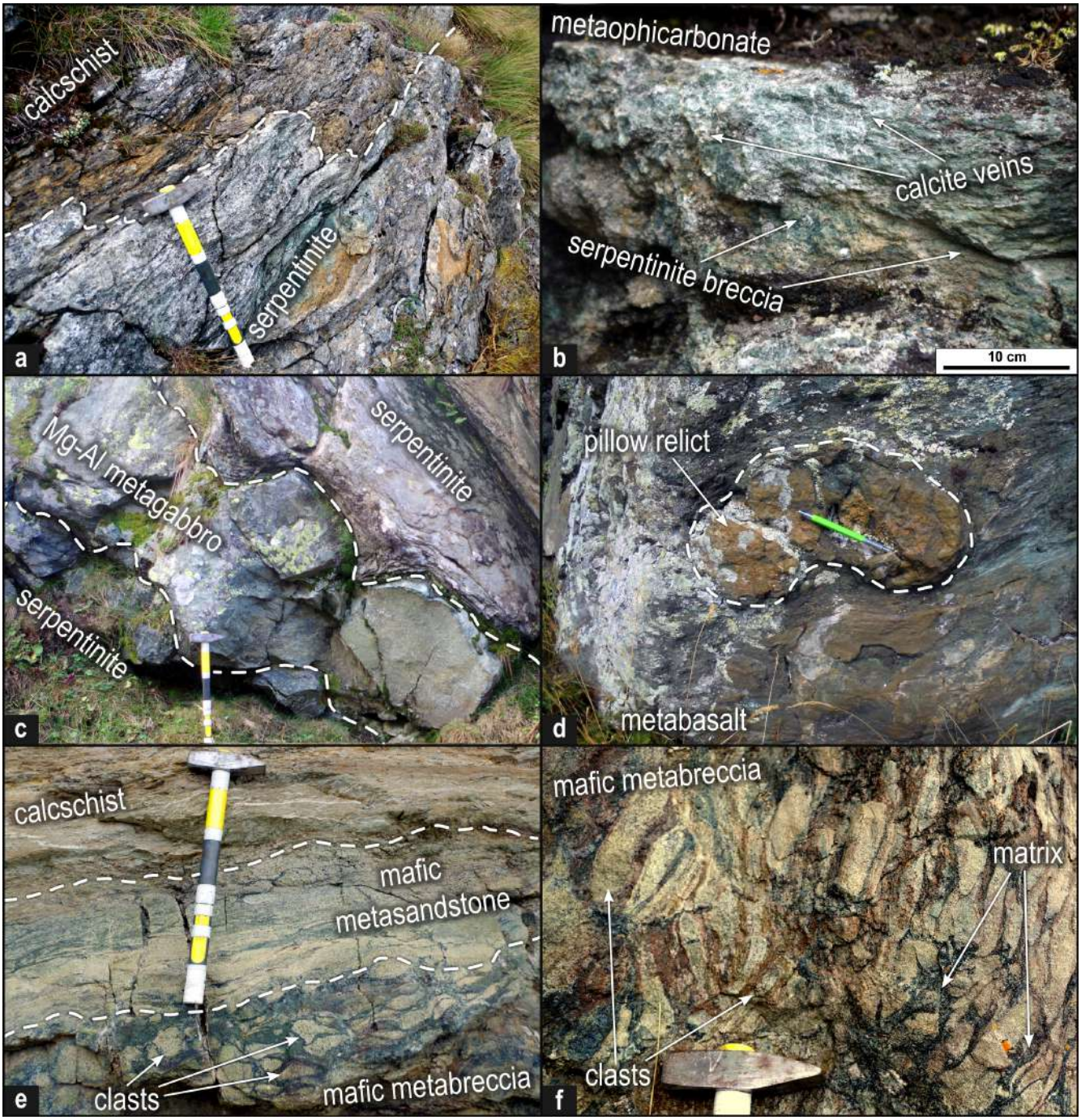

Figure 4. Field photographs of the main lithotypes , preserved primary stratigraphic contacts and relationships, and pre-alpine relict structures in the study area. (**a**) Folded stratigraphic contact between calcschist and serpentinite. 45°12′22.5″ N 7°09′10.6″ E. (**b**) Close-up view of metaophicarbonate horizon between serpentinite and calcschist, showing a brecciated structure as well as thin, anastomosing calcite veins. 45°12′23.2″ N 7°09′12.5″ E. (**c**) Boudinated Mg-Al metagabbro body embedded in foliated serpentinite. 45°12′24.3″ N 7°08′58.0″ E. (**d**) Metabasalt showing relicts of pillow structure inside a fine-grained mafic matrix. 45°11′42.9″ N 7°08′52.1″ E. (**e**) Mafic paraderivate horizon interlayered in calcareous calcschist, in which mafic metabreccia (made up of greenish sub-angular clasts and a bluish fine-grained matrix) passes upwards to medium- to fine-grained mafic metasandstone, which displays a relict graded texture. 45°12′25.9″ N 7°08′56.0″ E. (**f**) Detail of the relict texture in mafic metabreccia, highlighting the size and the shape of the recrystallized clasts, embedded in a fine grained matrix. 45°12′25.9″ N 7°08′56.0″ E.

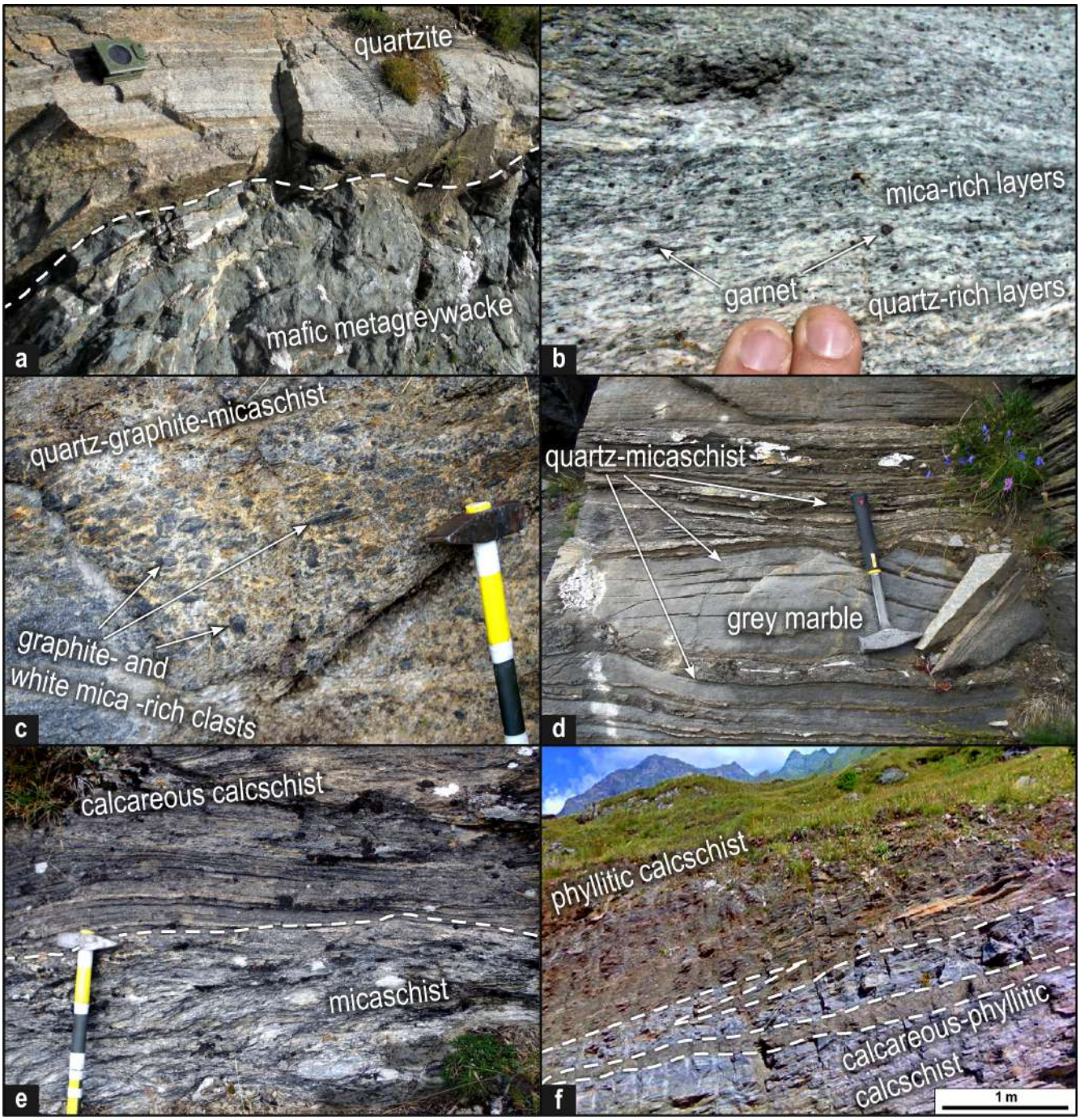

Figure 5. (**a**) Stratigraphic (primary) contact between mafic metagreywacke, with a relict clastic texture and secondary carbonate cement, and quartzite, characterized by a primary alternating of quartz-carbonate-mica (dark) levels and quartz (whitish) layers. 45°12′26.1″ N 7°09′15.1″ E. (**b**) Details of the garnet-bearing micaceous quartzite, showing different layers enriched in quartz (whitish levels) and white mica (grey levels), both studded of cm-sized garnet. 45°12′28.1″ N 7°09′01.6″ E. (**c**) Graphite-rich quartz-micaschist, showing several graphite- and white mica-rich irregular clast relicts. 45°12′32.4″ N 7°09′49.1″ E. (**d**) Gray marble with dm- to cm-sized quartz-bearing micaschist layers, representing the transitional contact between marble and underlying quartzite. 45°12′27.0″ N 7°09′33.0″ E. (**e**) Overturned contact between calcareous calcschist and micaschist. The former shows alternating cm-sized carbonate-rich and phyllosilicate-rich layers, which appear interrupted along the contact. Micaschist is enriched in quartz, showing a modest graphite (and rarely carbonate) content. 45°12′28.7″ N 7°08′44.3″ E. (**f**) Transitional stratigraphic contact between the phyllitic calcschist and the calcareous-phyllitic calcschist. 45°12′27.6″ N 7°08′54.9″ E.

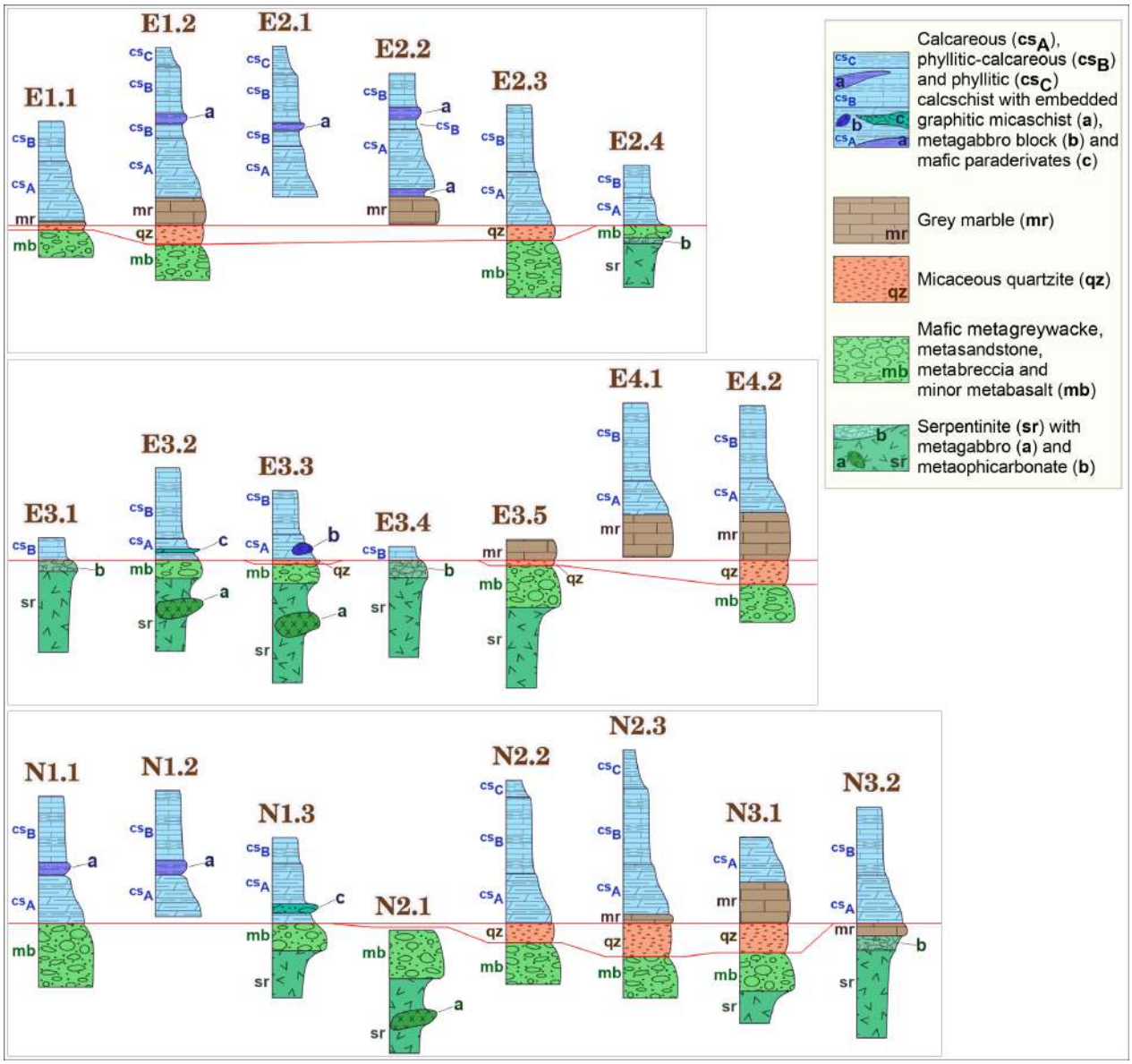

Figure 6. Lithostratigraphic columns (not to scale) reconstructed along the E–W (*E1* and *E2* above; *E3* and *E4* middle) and the N–S-oriented (*N1*, *N2*, and *N3* below) cross sections of Figures 2b and 3. The stratigraphic base of both gray marble and quarzite is correlated throughout all columns with a red line.

4. Lithostratigraphy of the IPZ

In the study area (Figure 2), the IPZ consists of a metaophiolitic basement, characterized by ultramafic (serpentinite) and mafic (metagabbro) rocks, and a heterogeneous metasedimentary supra-ophiolite cover, including detrital horizons with metabasite clasts, quartzite, and gray marble, which are followed by a thick calcschist succession.

Massive to schistose serpentinite, ranging from light to blackish green colors along with the magnetite content, is up to one-hundred meters thick and mainly crops out in the southeastern sector of the study area (Figure 2a). Serpentine and minor chlorite lamellae define the main foliation. This lithotype shows primary contacts with both metabasic rocks and the calcschist succession (Figure 4a). In the latter case, the contact is locally marked by horizons of ophicarbonate, serpentinite breccia (Figure 4b), and actinolite-chlorite-serpentine schist. Metadoleritic bodies, probably corresponding to primary dykes, occur within the serpentinite, displaying sharp contacts and a banding defined by epidote-rich and albite-chlorite-rich layers.

Metagabbro scarcely crops out in the study area, mainly occurring as elongated bodies, up to few meters in thickness, embedded within the serpentinite (Figure 4c). It consists of plagioclase, epidote, chlorite, and amphiboles, and it displays a massive to weakly foliated texture defined by amphibole and chlorite preferred orientations (locally underlined by a compositional banding).

Metabasic rocks are mainly represented by abundant mafic to intermediate paraderivates (mainly metagreywacke, metasandstone, and metabreccia) and by scarce metabasalt, ranging in thickness from centimeters to few hundreds of meters (south of Nero Lake, Figure 2a). Metabasalt occurs in the lowest portion of the sequence, showing massive and homogeneous structures, with few relicts of primary igneous textures, such as pillow-lavas with sub-lenticular geometry (Figure 4d).

The metabasalt is overlain by the metasedimentary cover, whose first terms consist of decimeter-thick horizons of metagreywacke, and matrix-to clast-supported metabreccia (Figures 4e,f and 5a) with angular to sub-rounded mafic clasts, up to few dm in size, in a fine-grained epidote-albite-bearing mafic to carbonate matrix. Internally, most of these detrital horizons show alternating fine- and medium- to coarse-grained levels of mafic composition, up to decimeters thick. Fine-grained levels show albite enrichments, while medium to coarser ones include sub-angular to sub-rounded and elongated recrystallized clasts mainly made of epidote, amphibole, and chlorite within a bluish amphibole-chlorite-rich matrix (Figure 4e,f). Some horizons are characterized by mm-to-cm-sized epidote-albite levels alternating with amphibole-chlorite bands, locally containing sub-rounded recrystallized clasts, suggesting a sedimentary origin which is consistent with mafic fine- to medium-grained metasandstone. Locally, metabasic rocks are represented by carbonate-bearing actinolitic schist and gabbroic metasandstone with graded structures, from coarse to medium grained clasts. Mafic paraderivates are enriched in phyllosilicates and carbonate, suggesting a sedimentary origin.

The above-described lithostratigraphy is overlain by the supra-ophiolitic metasedimentary cover consisting of different types of quartzite, up to a few meters in thickness, which differ each other's in the quartz-phyllosilicate relative abundance (Figure 5a–c). Pure fine-grained quartzite layers, dm- to m-thick, locally drape the top of the metabasic rocks. The most widespread quartzite type, instead, is a light gray garnet-bearing micaceous quartzite (Figure 5b). This is internally characterized by the occurrence of some cm-sized dark-colored layers shown by the abundance of very fine-grained accessory minerals (Figure 5a), thin carbonate-bearing layers, and sub-rounded quartz-mica aggregates, mm- to cm in size, which could represent clasts or primary boudins. These features and the difference in grain size among levels define a banded texture (locality Gr.e Ciape in Figure 2a). Locally, a quartz-graphite-rich micaschist occurs above or laterally to the quartzite, showing transitional vertical to lateral (Figure 5c) contacts. Mica-quartz-graphite rounded aggregates, up to centimeters in size, also occur within those levels, representing former clasts or primary boudinated layers.

All the lithostratigraphic units and rocks of the IPZ described above are overlain by a thick calcschist succession, suggesting that its base corresponds to an unconformity surface. From the bottom upwards, the calcschist succession consists of three different members, showing transitional primary contacts between them as well as thickness variations: (I) calcareous calcschist, (II) calcareous-phyllitic calcschist, and (III) phyllitic calcschist. Although the complex structural setting and the lack of continuous stratigraphical markers, the total thickness of each member, as well as the whole calcschist succession, is difficult to be defined in detail but it can be evaluated around few hundred meters.

The carbonate content increases upward in the lithostratigraphic units and the quartzite gradually passes to a discontinuous gray marble, which, however, locally directly overlays both metabasic and mantle rocks, such as in the Gr.e Castelletto and Gr.e Ciape sectors (Figure 2a). The gray marble is a chlorite-bearing micaceous calcite marble (Figure 5d) with minor amounts of quartz and, locally abundant, cm-sized tourmaline crystals. It ranges in thickness from few decimeters to one hundred meters.

The **calcareous calcschist** member, up to about 100 m in thickness, consists of alternating few centimeters thick levels of medium-grained calcite with minor quartz, white mica, and chlorite, locally containing garnet and tourmaline porphyroblasts. Often, quartz-rich thin levels are observed. Phyllite-micaschist lenses, up to centimeters thick, frequently occur in levels within the calcareous calcschist, representing primary clasts or boudins.

A lenticular body of graphitic micaschist, several meters in thickness, locally crops out (i.e., near Nero Lake, see Figure 2a) at the base of this member, marking the contact with the underlying gray marble. It consists of alternating garnet-rich graphitic micaschist and quartz-micaschist layers, up to decimeters in thickness, with thinner micaceous graphite-bearing quartzite levels. Some mafic metagreywacke, metaconglomerate, and metasandstone horizons, up to decimeters thick, are also interfingered within the calcareous calcschist member and are locally followed by thin quartz-rich levels. At the same tectono-stratigraphic level, a block of metagabbro, a few meters wide, crops out along the Stura di Viù River, East of Malciaussia Lake (see Figure 2a).

The **calcareous-phyllitic calcschist** member is composed of calcite, white mica, chlorite, and quartz, and it ranges in thickness from 100 to 150 m, tapering out toward those sectors where the underlying calcareous calcschist member is reduced or absent (see Figures 2a and 3). Inside this member (and locally at its contact with calcareous calcschist, Figure 5e) few discontinuous levels of graphitic micaschist, up to some meters thick, also occur.

The calcareous-phyllitic calcschist member gradually passes upward to the **phyllitic calcschist** member (Figure 5f), according to the increase of phyllosilicates content. The latter consists of thick phyllosilicate levels with abundant quartz, alternating with thin poorly carbonate phyllite levels. Graphite is almost the ubiquitarian component, resulting in the dark gray color and the shiny appearance of these metasedimentary unit. In the upper part of the member, a m-thick polymictic discontinuous metaconglomerate body occurs, showing clasts of metabasic rocks, micaschist, and marble mm-to dm in size and rounded to elongated in shape, embedded in a carbonate-phyllitic matrix.

5. Alpine Structural Evolution

The IPZ succession is deformed by four main alpine ductile phases, from D1 to D4. The first phase (D1) is preserved only in the more competent lithologies, where it corresponds to the oldest tectono-metamorphic foliation (S1), also representing the axial plane of isoclinal folds. The D2 deformation phase developed large-scale (hundreds of meters) isoclinal folds (Figures 2a and 3), whose S2 pervasive axial plane foliation corresponds to the regional foliation, N-NW plunging. Both D1 and D2 phases developed sheath folds, which are well documented at all scales by anvil- or eye-shaped folds, such as the map-scale one occurring in the calcschist to the south of Lake Nero (see Figure 2a and the *N2* insert in Figure 3). Along the D2 folds limbs, the parallelism between S1 and S2 defines a composite S1 + S2 fabric. The D3 phase developed open to closed folds, whose axial plane is locally defined by crenulation cleavage in weaker lithologies. The D4 phase developed open to gentle folds, locally with kink geometry and axial plane defined by disjunctive cleavage.

The tectonic contact between the IPZ and the overlying EPZ consists of a thick shear zone (see Figures 1b and 2), which represents the northern prosecution of the Susa Shear Zone (sensu Ghignone et al. [35], Gasco et al. [60], Ghignone et al. [65]). It is characterized by a tectonic mélange-like blocks-in-matrix structure (see [69]), with huge exotic blocks of metabasite, serpentinite, and marble embedded in a mylonitic calcschist matrix, and records a first shear event with top-to-E sense of shear reactivated by top-to-W sense of shear. The mylonitic foliation is deformed by the D3 and D4 regional deformation phases.

6. Discussion

Although the pervasive overprinting of Alpine tectonic deformation and metamorphism is present, detailed geological mapping (Figure 2) and structural and stratigraphical observations (Figures 3 and 6) allow us to recognize remnants of an original intra-oceanic

(pre-orogenic) stratigraphic succession (Figure 6) in the IPZ of the Stura di Viù Valley, which also preserves primary stratigraphic contacts between different lithotypes as well as some relict primary textures and structures. The reconstruction of the structural setting through several N–S- and E–W-oriented cross sections (Figure 3) shows that the stratigraphic succession, which consists of a metaophiolite basement followed by syn-extensional and post-extensional metasediments, is characterized by a strong lateral and vertical heterogeneity.

In the following, we discuss the character and tectono-stratigraphic significance (Section 6.1) of this heterogeneous succession in order to reconstruct the intra-oceanic (pre-orogenic) physiography of this sector of the Alpine Tethys (Section 6.2).

6.1. The Intra-Oceanic Stratigraphy of the IPZ Metaophiolite

Above the mantle rocks, the lateral and vertical correlations among different selected and representative litostratigraphic columns (Figure 6) that we have reconstructed from both field observations (Figure 2) and cross sections (Figure 3) allow documenting, in detail, the heterogeneity of the stratigraphic succession. These correlations outline that below the calcschist, two different successions (Figure 7), differing each to other in their completeness, characterize different sectors of the studied area.

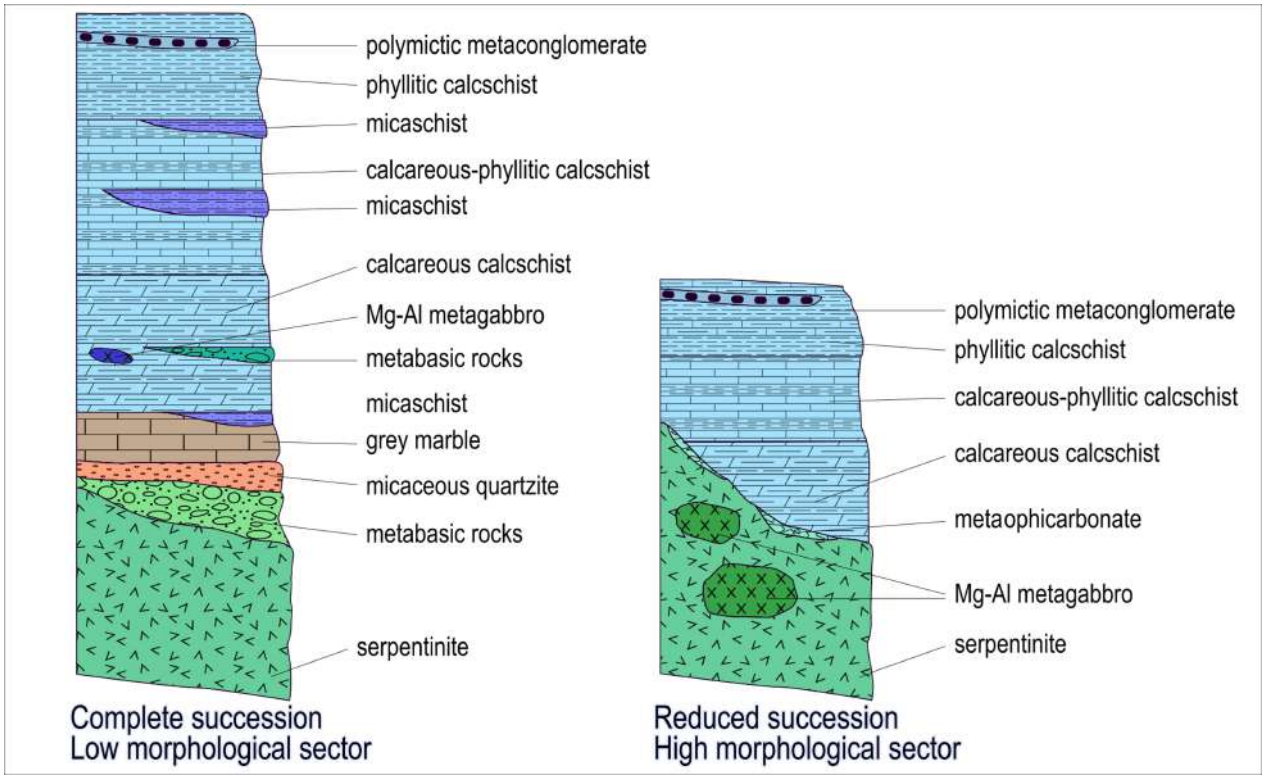

Figure 7. Stratigraphic columns of the "complete" and "reduced" successions, reconstructed from field data.

Sectors to the east and SE of the Nero Lake and to the west of the Malciaussia Lake are characterized by a "complete" stratigraphic succession (Figures 2a and 7) which is defined by the occurrence of all the terms of the lithostratigraphic succession (i.e., mafic metabreccia and metasandstone, quartzite, and marble) above the mantle rocks. The latter consist of serpentinite with rare metagabbro intrusions and no ophicalcite horizons. Mafic metasandstone is prevalent with respect to the mafic metabreccia, and locally they are absent (Figures 2a, 3 and 6). On the contrary, sectors to the east of the Malciaussia Lake and to the south of the Nero Lake are characterized by a "reduced" stratigraphic succession (Figures 2a and 7), which is defined by the unconformable contact of the calcschist above the mantle rocks, lacking quartzite and gray marble. In these sectors, the

serpentinite is commonly intruded by metagabbro bodies, while its top is characterized by thick ophicalcite horizons. Mafic metabreccias is prevalent, showing a gradual transition to mafic metagreywake and metasandstone towards sectors where the "complete" succession is exposed (Figures 2a, 3 and 6). Toward the same directions, the "complete" succession tapers out up to disappear, with the marble and quartzite elision (see, e.g., *E1.1*, *E2.3*, *E3.3*, *N2.2* and *N3.2* in Figure 6).

Furthermore, the calcschist shows vertical and lateral variations above the "complete" and "reduced" successions. Above the former, the calcschist is commonly characterized by the occurrence of all the three members or at least two when the uppermost one is absent (see, e.g., *E1.2*, *E2.1*, *E2.3*, *E4.2*, and *N2.3* in Figure 6). On the contrary, in sectors where the "reduced" succession prevails, the calcschist sequence locally lacks the lower member (i.e., the calcareous calcschist member; see, e.g., *E3.1* and *E3.4* in Figure 6).

6.2. Reconstruction of the Intra-Oceanic Seafloor Physiography

In the metaophiolite basement, the occurrence of Mg-Al metagabbro bodies (Figure 2a, and *E2.4*, *E3.2*, *E3.3*, and *N2.1*, in Figure 6) likely corresponds to shallow intrusions of mafic melts (such as dykes and more irregular intrusive lenticular bodies) in the upper mantle peridotites as documented during the main magmatic event, which commonly predates the upper mantle exhumation (see, e.g., in [7,70,71]). The hosting serpentinite represents the widespread serpentinization of the former peridotite, which is commonly attributed to seawater interaction during mantle exhumation on the ocean floor.

Ophicarbonate horizons at the top of the serpentinite document a period of mantle rocks exposure on the ocean floor during which brittle deformation facilitated hydrothermal fluid circulation (see, e.g., in [21,72,73]). In the same sites, evidences that calcschist directly overlies both mantle rocks and ophicarbonate horizons (*E3.1*, *E3.3*, and *N3.2* in Figure 6) suggest that these sectors likely corresponded to morphological or structural highs within the depositional basin, where the "reduced" succession deposited (Figures 7 and 8).

The existence of this articulated seafloor topography, with such morphological or structural highs, is also supported by the occurrence of mafic metabreccia, metagreywacke, and metasandstone resting directly above both serpentinized mantle and pillow metabasalt (Figures 7 and 8). Although partially reworked and deformed by Alpine-related tectonics and metamorphic recrystallization, the preserved sedimentological characteristics and textures of those detrital units suggest they represent the product of downslope transformation from hyperconcentrated flows (e.g., matrix- and clast-supported breccia) to turbidity currents (e.g., greywacke and sandstone). The very poorly sorted and clastic texture of mafic metabreccia document deposition proximal to the source area (i.e., along or at the base of the scarp), according to a reduced downslope transport, while the most sorted and finer-grained mafic metagreywacke and metasandstone document deposition in a more distal sector (i.e., from base of the scarp to proximal basin). The lack of metabasalt rocks cropping out in the morphological or structural highs suggests that the source area for this mafic detrital material was located outside of the studied sector, even if very close to it. Alternatively, this source may have been completely eroded from morphological or structural highs, although less probable. The occurrence of quartzite and gray marble above the mafic metabreccia, metagreywacke and metasandstone represents the deposition of a "complete" succession (Figure 7) in a basinal sector (i.e., morphological or structural low) of the articulated seafloor topography with respect to the source area of detrital material (i.e., morphological or structural highs).

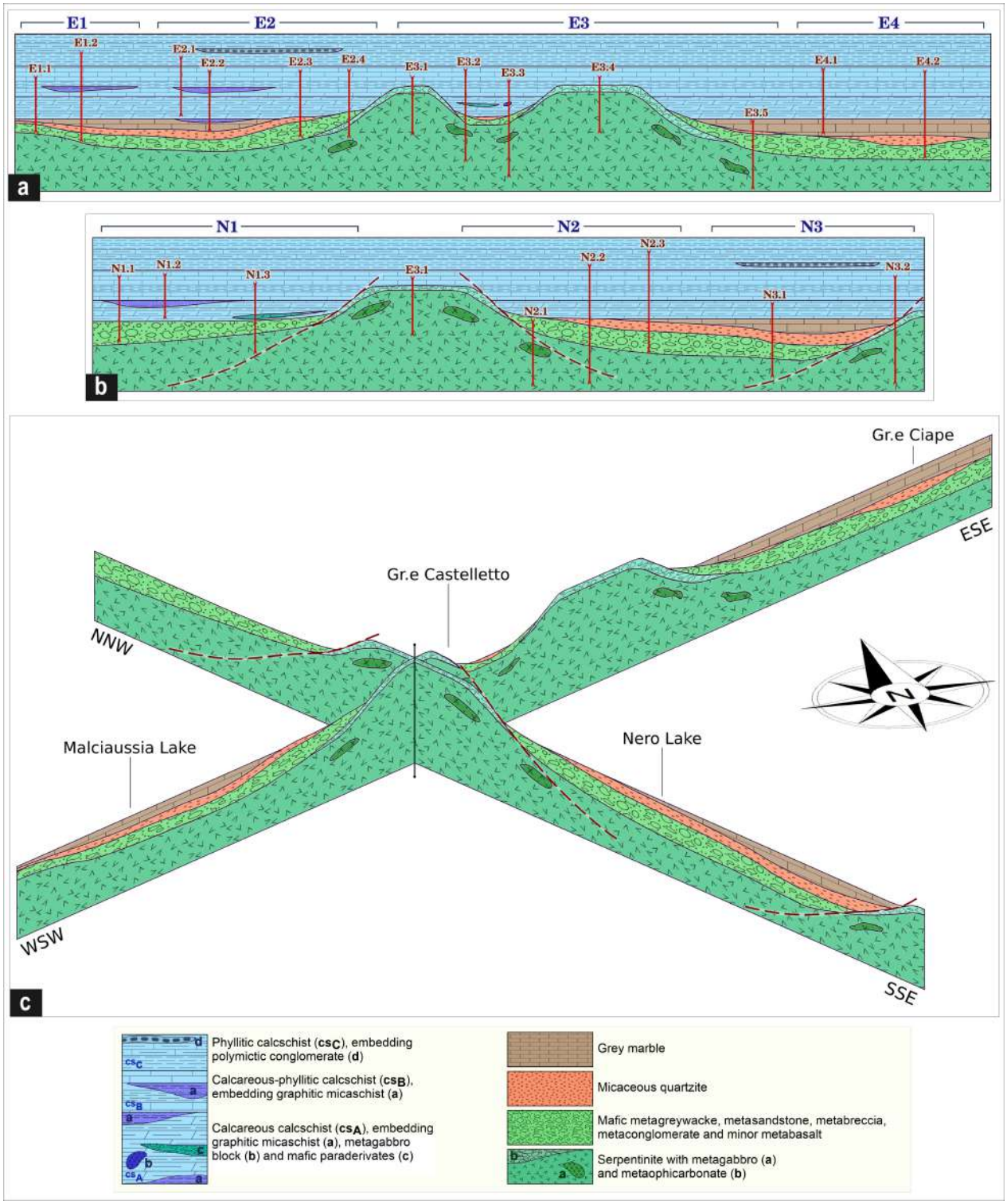

Figure 8. Simplified E–W (**a**) and N–S (**b**) striking reconstructions (not to scale) of the intra-oceanic (pre-orogenic) tectono-stratigraphic seafloor architecture of the Alpine Tethys in the studied sector at time of calcschist deposition (i.e., Late Cretaceous–Early Palaeocene?). Dark red dotted lines show the position of inferred faults, bounding high sectors. The red vertical lines show the position of the lithostratigraphic columns of Figure 6 (see text for details). (**c**) Fence diagram showing the lateral and vertical heterogeneities within the reconstructed Jurassic succession of the Alpine Tethys in the IPZ. The whole calcschist succession has been omitted to better show the inherited Jurassic basin floor physiography. The black central vertical line represents the *E3.1* lithostratigraphic column, which is present in both the sections.

The quartzite represents the first pelagic siliceous deposit, mainly laying on mafic metabreccias, metagreywacke, and metasandstone (*E3.5* and *N2.3* in Figure 6) but locally resting directly on the serpentinite in primary contact (*N3.2* in Figure 6). Its banded texture suggests a very pure siliceous deposit, which is well comparable with the Middle Bathonian to Early Callovian radiolarian chert of the Northern Apennines and Queyras Complex in the Western Alps (see, e.g., in [7,13,14,39,74–76]). The local occurrence (locality Gr.e Ciape in Figure 2a) above the lower part of the quartzite of supposed clasts made of quartz-mica aggregates and lithologic variations defined by intercalations of phyllosilicates-rich levels and/or containing impurities suggests that these sectors represent proximal basin portions where detrital material coming from morphological or structural highs reached the depositional area. The occurrence of thin micaceous quartzite and micaschist levels within the quartzite may represent primary intercalations of quartz-arenite and pelite, respectively, likely corresponding to turbidite inputs. Thin marble levels in the uppermost part of the quartzite document the gradual depositional change in the oceanic basin, which marks the transitional contact from quartzite to the above gray marble (Figure 8).

The distribution of marble is similar to that one of quartzite, representing deposition in pelagic environment, far from morphological or structural highs (Figure 8). Its compositional characteristics and stratigraphic position above the quartzite and below the calcschist succession suggest a close comparison with the Calcari a Calpionella of the non-metamorphosed Northern Apennines (see, e.g., in [14,74,76]) and the white marble of the blueschist-facies Queyras Complex (see, e.g., in [7,9,39,75]), which is Tithonian to Berriasian in age (i.e., between c. 152 and 140 Ma). A comparable whitish marble is also described in the eclogite-facies Monviso metaophiolite Complex by Balestro et al. [7]. These two lithostratigraphic units represent the onset of the post-extensional succession associated to the rifting stage. Particularly, the unconformity at the base of the gray marble marks the temporal boundary between the lithospheric-scale extension and a period of tectonic quiescence, during which pelagic deposition took place in and across the Alpine Tethys as documented from both the Northern Apennines (see, e.g., in [14,76]) and the Western Alps (see, e.g., in [7,15] and references therein).

The features of the thick calcschist succession, which shows an upward gradual decrease in the carbonate content from the lowermost to the uppermost members, document a gradual deepening of the depositional environment. The occurrence of minor quartz within the calcareous calcschist member agrees well with deposition of distal mixed carbonate-siliciclastic turbidites sourced from a continental margin area. However, the occurrence of mafic metagreywacke intercalations (*E3.1*; Figure 6) and of an isolated block (*E3.3*; Figure 6) of metagabbro documents that oceanic reliefs, consisting of mantle rocks, still emerged from the seafloor. The gradual increasing of phyllosilicate content within the overlying calcareous-phyllitic calcschist and the phyllitic calcschist members documents deposition of a distal turbidite system. The widespread occurrence of graphite as ubiquitarian component also suggests that high organic content characterized the depositional basin at this stage, as also documented by the occurrence of discontinuous lenticular bodies of graphitic micaschist, up to some meters thick, at different stratigraphic levels within the whole calcschist succession.

The intercalation within the phyllitic calcschist member of a metaconglomerate horizon, with mixed continental and oceanic clasts (metabasite, micaschist and marble), suggests gravitational flows likely sourced from the accretionary wedge during the convergent stage.

The different lithostratigraphic characteristics of the lower (i.e., calcareous calcschist) and the two overlying (i.e., calcareous-phyllitic calcschist and the phyllitic calcschist) members of the calcschist succession show a good comparison with the Replatte Formation and Roche Noir Formation, respectively, of the blueschist Queyras Complex in the EPZ (see, e.g., in [39,75]). The two latter formations of the Queyras Complex were classically compared with the non-metamorphosed Palombini Shale (Early to Late Cretaceous) and Val Lavagna Schist Group (Late Cretaceous) of the Northern Apennines (see, e.g., in [7,13,14,77]), respec-

tively. Differently from the Northern Apennines, where mantle rock olistoliths (i.e., blocks of gravitational origin) are not present within the Palombini Shale (e.g., [76]), the occurrence of the gabbro block within the lower member of the calcschist succession may suggest that topographic or structural mantle reliefs characterized the seafloor of the studied sector during the Early–Late Cretaceous period. Uplifted mantle ridges were, however, documented to characterize the intra-oceanic seafloor topography of the Ligurian-Piedmont oceanic basin of the present-day Northern Apennines since Cenomanian time (see the "Ruga del Bracco" in [78]) where Palombini Shales directly lies above mantle rocks, at least locally (see, e.g., in [14]). The occurrence of mafic metagreywake intercalations within the same calcschist member hosting the metagabbro block thus seems to exclude a tectonic origin for this block occurrence, even if additional analyses are necessary to better support our interpretation.

Moreover, on the basis of their compositional features and stratigraphical position, the metaconglomerate horizons within phyllitic calcschist could be tentatively correlated with the Bocco Shale (Early Palaeocene?) from Northern Apennines (see, e.g., in [79,80]).

7. Conclusions

Our detailed geological mapping, structural, and stratigraphical observations allowed us to reconstruct the intra-oceanic stratigraphy and tectono-sedimentary depositional setting of the Jurassic Alpine Tethys for the sector presently corresponding to the IPZ metaophiolite of the Stura di Viù Valley (Lanzo Valleys), in the axial zone of the eclogite facies Western Alps. Our findings document that the character of the stratigraphic succession shows, in general, a good comparison with both the oceanic succession of the Queyras Complex in the External Piedmont Zone (EPZ) of Western Alps (see, e.g., in [7,9,39,75]) and the Internal Ligurian Units in the Northern Apennines (see, e.g., in [14,74,76]), ranging from Middle Jurassic to Late Cretaceous in age.

This metaophiolite succession, which consists of a serpentinized mantle with rare metagabbro intrusions and metabasalt effusions followed by a heterogeneous metasedimentary cover, is characterized by significant variations in both thickness and facies. Variations reflect a strongly articulated seafloor physiography and mantle–sediment interface, resulting from tectono-stratigraphic processes related to the Middle to Late Jurassic seafloor spreading stage and mantle exhumation. Mafic metabreccia and metasandstone above the serpentinized mantle with gabbro intrusions represent a syn-extensional deposit, ranging from hyperconcentrated flows to turbidite currents, whose distribution marked the physiography of slope sectors connecting morphological or structural highs and lows within the basin. However, the source area of these mafic detrital materials was likely outside of the studied area, even if close to it, because the reconstructed morphological or structural high sectors in the studied area are devoid of exposed metabasite rocks.

The reconstructed metaophiolite succession shows a close similarity with the tectono-stratigraphic settings observed in modern slow-spreading (Atlantis Massif, Mid-Atlantic Ridge-MAR) and the ultraslow-spreading (Atlantis Bank, Southwest Indian Ridges (SWIR)) mid-ocean ridges (see, e.g., in [1–4,6]), fundamentally differing from those Penrose-type [81] and subduction-influenced suprasubduction-zone ophiolites (e.g., Troodos in Cyprus, Semail-Oman in Oman, and Mirdita in Albania). Moreover, the scarcity of preserved lavas and the great abundance of reworked mafic products directly above the exhumed mantle allow us to refer this metaophiolite to the "continental margin type" of Dilek and Furnes [82].

"Complete" and "reduced" successions were recognized, documenting deposition in morphological or structural lows and highs, respectively. The articulated seafloor physiography was gradually smoothed by deposition of quartzite and gray marble, which represent the post-extensional succession (see, e.g., in [7]). However, isolated mantle reliefs persisted during the calcschist deposition. The occurrence of quartz-rich levels within the lower calcschist member (i.e., the calcareous calcschist member), as well as that one of the graphitic micaschist intecalations, suggests that the deposition setting received material

sourced from the erosion of a continental margins since the Early Cretaceous. The mixed oceanic and continental clasts of the metaconglomerate horizon in the uppermost member of the calcschist succession (i.e., the phyllitic calcschist member), which is well comparable with Late Cretaceous sediments of the Queyras Complex (see, e.g., in [7,9,39,75]) and Northern Apennines (see, e.g., in [14,74,76]), probably document the onset of the convergence stage.

In conclusion, our results may provide significant tectono-stratigraphic constraints to take into consideration for a better understanding of the Western Alpine evolution. In fact, it is well documented that the occurrence of both a heterogeneous stratigraphic succession, with its internal rheological contrasts, and an articulated tectono-stratigraphic architecture of the depositional setting, represent, among others, important inheritance elements which may provide ideal conditions to nucleate tectonic and rheological weakness zones that can drive deformation during the subsequent convergent stage (see, e.g., in [17,18,21–30]).

Supplementary Materials: The following are available online at https://www.mdpi.com/2075-163X/11/4/361/s1. Figure S1: Simplified geological map of the study area showing the location of well-preserved primary lithostratigraphic relationships, used for lithostratigraphic columns reconstruction.

Author Contributions: Conceptualization, M.D.T., M.G. and S.G.; methodology, M.D.T., M.G. and S.G.; validation, M.G., S.G. and A.F.; formal analysis, M.D.T., M.G. and S.G.; investigation, M.D.T., M.G. and S.G.; resources, M.D.T. and M.G.; data curation, M.D.T. and S.G.; writing—original draft preparation, M.D.T.; writing—review and editing, M.D.T., M.G., S.G. and A.F.; visualization, M.D.T.; supervision, M.G. and S.G.; project administration, M.G. All authors have read and agreed to the published version of the manuscript.

Funding: This work was supported by research grants from University of Torino, Ricerca Locale "ex 60%" 2018–2020 (M.G., S.G., and A.F.).

Institutional Review Board Statement: Not applicable.

Informed Consent Statement: Not applicable.

Data Availability Statement: All data generated or analyzed during this study are included in this published article.

Acknowledgments: We thank Guest Editors P. Tartarotti and E. Cannaò and Assistant Editor N. Burazer for the careful editorial handling and the three anonymous reviewers for their constructive and thorough reviews.

Conflicts of Interest: The authors declare no conflict of interest.

References

1. Cannat, M. Emplacement of mantle rocks in the seafloor at mid-ocean ridges. *J. Geophys. Res. Solid Earth* **1993**, *98*, 4163–4172. [CrossRef]
2. Karson, J.; Lawrence, R. Tectonic setting of serpentinite exposures on the western median valley wall of the MARK Area in the vicinity of Site 920. In *Proceedings of the Ocean Drilling Program, Scientific Results*; Karson J.A., Cannat M., Miller D.J., Elthon D., Eds.; Texas A&M University: College Station, TX, USA, 1997; Volume 153, pp. 5–22.
3. Tucholke, B.; Lin, J.; Kleinrock, M. Megamullions and mullion structure defining oceanic metamorphic core complexes on the Mid-Atlantic Ridge. *J. Geophys. Res. Solid Earth* **1998**, *103*, 9857–9866. [CrossRef]
4. MacLeod, C.; Searle, R.; Murtonc, B.; Casey, J.; Mallows, C.; Unsworth, S.; Achenbach, K.; Harris, M. Life cycle of oceanic core complexes. *Earth Planet. Sci. Lett.* **2009**, *287*, 333–344. [CrossRef]
5. Manatschal, G.; Sauter, D.; Karpoff, A.; Masini, E.; Mohn, G.; Lagabrielle, Y. The Chenaillet Ophiolite in the French/Italian Alps: An ancient analogue for an Oceanic Core Complex? *Lithos* **2011**, *124*, 3–4. [CrossRef]
6. Escartín, J.; Mével, C. Tectonic structure, evolution, and the nature of oceanic core complexes and their detachment fault zones (13°20′ N and 13°30′ N, Mid Atlantic Ridge). *Geochem. Geophys. Geosyst.* **2017**, *18*, 1451–1482. [CrossRef]
7. Balestro, G.; Festa, A.; Dilek, Y. Structural architecture of the Western Alpine Ophiolites, and the Jurassic seafloor spreading tectonics of the Alpine Tethys. *J. Geol. Soc.* **2019**, *176*, 913–930. [CrossRef]
8. Varga, R.; Moores, E. Spreading structure of the Troodos ophiolite, Cyprus. *Geology* **1985**, *13*, 846–850. [CrossRef]
9. Lemoine, M.; Tricart, P.; Boillot, G. Ultramafic and gabbroic ocean floor of the Ligurian Tethys (Alps, Corsica, Apennines): In search of a genetic model. *Geology* **1987**, *15*, 622–625. [CrossRef]
10. Harper, G. Episodic magma chambers and amagmatic extension in the Josephine ophiolite. *Geology* **1988**, *16*, 831–834. [CrossRef]

11. Froitzheim, N.; Gregor, E. Extensional detachment faulting in the evolution of a Tethys passive continental margin, Eastern Alps, Switzerland. *Geol. Soc. Am. Bull. Front.* **1297–1308**, *102*, 167–188. [CrossRef]
12. Dilek, Y.; Eddy, C. The Troodos (Cyprus) and Kizildag (S. Turkey) Ophiolites as Structural Models for Slow-Spreading Ridge Segments. *J. Geol.* **1992**, *100*, 305–322. [CrossRef]
13. Lagabrielle, Y. Ophiolites of the southwestern Alps and the structure of the Tethyan oceanic lithosphere. *Ofioliti* **1994**, *19*, 413–434.
14. Principi, G.; Bortolotti, V.; Chiari, M.; Cortesogno, L.; Gaggero, L.; Marcucci, M.; Saccani, E.; Treves, B. The pre-orogenic volcano-sedimentary covers of the western Tethys oceanic basin: A review. *Ofioliti* **2004**, *29*, 177–211.
15. Balestro, G.; Lombardo, B.; Vaggelli, G.; Borghi, A.; Festa, A.; Gattiglio, M. Tectonostratigraphy of the northern Monviso meta-ophiolite complex (Western Alps). *Ital. J. Geosci.* **2014**, *133*, 409–426. [CrossRef]
16. Clerc, C.; Lagabrielle, Y. Thermal control on the modes of crustal thinning leading to mantle exhumation: Insights from the Cretaceous Pyrenean hot palaeomargins. *Tectonics* **2014**, *33*, 1340–1359. [CrossRef]
17. Festa, A.; Balestro, G.; Borghi, A.; De Caroli, S.; Succo, A. The role of structural inheritance in continental break-up and exhumation of Alpine Tethyan mantle (Canavese Zone, Western Alps). *Geosci. Front.* **2020**, *11*, 167–188. [CrossRef]
18. Lagabrielle, Y.; Asti, R.; Duretz, T.; Clerc, C.; Fourcade, S.; Teixell, A.; Labaume, P.; Corre, B.; Saspiturry, N. A review of Cretaceous smooth-slopes extensional basins along the Iberia-Eurasia plate boundary: How pre-rift salt controls the modes of continental rifting and mantle exhumation. *Earth-Sci. Rev.* **2020**, *201*, 103071. [CrossRef]
19. Girardeau, J.; Mével, C. Amphibolitized sheared gabbros from ophiolites as indicators of the evolution of the oceanic crust: Bay of Islands, Newfoundland. *Earth Planet. Sci. Lett.* **1982**, *61*, 151–165. [CrossRef]
20. Schroeder, T.; John, B.; Frost, B. Geologic implications of seawater circulation through peridotite exposed at slow-spreading mid-ocean ridges. *Geology* **2002**, *30*, 367–370. [CrossRef]
21. Tartarotti, P.; Guerini, S.; F., F.R.; Festa, A.; Balestro, G.; Bebout, G.; Cannaò, E.; Epstein, G.; Scambelluri, M. Superposed sedimentary and tectonic block-in-matrix fabrics in a subducted serpentinite mélange (High-Pressure Zermatt Saas Ophiolite, Western Alps). *Geosciences* **2019**, *9*, 358. [CrossRef]
22. Toth, J.; Gurnis, M. Dynamics of subduction initiation at preexisting fault zones. *J. Geophys. Res.* **1998**, *103*, 18053–18067. [CrossRef]
23. Tommasi, A.; Vauchez, A. Continental rifting parallel to ancient collisional belts: An effect of the mechanical anisotropy of the lithospheric mantle. *Earth Planet. Sci. Lett.* **2001**, *185*, 199–210. [CrossRef]
24. Hall, C.; Gurnis, M.; Sdrolias, M.; Lavier, L.; Muller, R. Catastrophic initiation of subduction following forced convergence across fracture zones. *Earth Planet. Sci. Lett.* **2003**, *212*, 15–30. [CrossRef]
25. Leng, W.; Gurnis, M. Dynamics of subduction initiation with different evolutionary pathways. *Geochem. Geophys. Geosyst.* **2011**, *12*, Q12018. [CrossRef]
26. Spalla, M.; Zanoni, D.; Marotta, A.; Rebay, G.; Roda, M.; Zucali, M.; Gosso, G. The transition from Variscan collision to continental break-up in the Alps: Insights from the comparison between natural data and numerical model predictions. In *The Variscan Orogeny: Extent, Timescale and the Formation of the Europe*; Schulmann, K., Martínez Catalán, J.R., Lardeaux, J.M., Janousek, V., Oggiano, G., Eds.; Geological Society, London, Special Publications: London, UK, 2014; Volume 405, pp. 363–400.
27. Balestro, G.; Festa, A.; Borghi, A.; Castelli, D.; Tartarotti, P.; Gattiglio, M. Role of late Jurassic intra-oceanic structural inheritance in the Alpine tectonic evolution of the Monviso meta-ophiolite complex (Western Alps). *Geol. Mag.* **2018**, *155*, 233–249. [CrossRef]
28. Marotta, A.; Roda, M.; Conte, K.; Spalla, M. Thermo-mechanical numerical model of the transition from continental rifting to oceanic spreading: The case study of the Alpine Tethys. *Geol. Mag.* **2018**, *155*, 250–279. [CrossRef]
29. Roda, M.; Regorda, A.; Spalla, M.; Marotta, A. What drives Alpine Tethys opening? Clues from the review of geological data and model predictions. *Geol. J.* **2019**, *54*, 2646–2664. [CrossRef]
30. Rotondo, F.; Tartarotti, P.; Guerini, S.; Della Porta, G.; Campomenosi, N. Metasomatic horizon sealing serpentinite-metasediments pair in the Zermatt-Saas metaophiolite (Northwestern Alps): Record of a channel for focused fluid flow during subduction. *Ofioliti* **2021**, *46*, 1–25.
31. Balestro, G.; Festa, A.; Dilek, Y.; Tartarotti, P. Pre-Alpine Extensional Tectonics of a Peridotite-Localized Oceanic Core Complex in the Late Jurassic, High-Pressure Monviso ophiolite (Western Alps). *Episodes* **2015**, *38*, 266–282. [CrossRef]
32. Nicolas, A. Le complexe Ophiolites-Schistes Lustrés entre Dora Maira et Grand Paradis (Alpés Piémontaises). Master's Thesis, University of Grenoble, Grenoble, France, 1966; p. 299.
33. Perotto, A.; Salino, C.; Pognante, U.; Genovese, G.; Gosso, G. Assetto geologico-strutturale della Falda Piemontese nel settore dell'alta Valle di Viù (Alpi occidentali). *Mem. Della Soc. Geol. Ital.* **1983**, *26*, 479–483.
34. Bigi, G.; Cosentino, D.; Parotto, M.; Sartori, R.; Scandone, P. Structural Model of Italy (1:500.000), CNR-Progetto finalizzato geodinamica (1:500.000). *Quad. Ric. Sci.* **1990**, Sheets I-II-III-IV. Available online: https://www.socgeol.it/438/structural-model-of-italy-scale-1-500-000.html (accessed on 26 February 2021).
35. Ghignone, S.; Gattiglio, M.; Balestro, G.; Borghi, A. Geology of the Susa Shear Zone (Susa Valley, Western Alps). *J. Maps* **2020**, *16*, 1–8. [CrossRef]
36. Ernst, W.; Dal Piaz, G. Mineral parageneses of eclogitic rocks and related mafic schists of the Piemonte ophiolite nappe, Breuil-St. Jacques area, Italian Western Alps. *Am. Mineral.* **1978**, *63*, 621–640.
37. Lemoine, M.; Tricart, P. Les Schistes Lustrés piémontais des Alpes Occidentales: Approche stratigraphique, structurale et sédimentologique. *Eclogae Geol. Helv.* **1986**, *79*, 271–294.

38. Vissers, R.; van Hinsbergen, D.; Meijer, P.; Piccardo, G. Kinematics of Jurassic ultra-slow spreading in the Piemonte Ligurian ocean. *Earth Planet. Sci. Lett.* **2013**, *380*, 138–150. [CrossRef]
39. Lemoine, M. Données nouvelles sur la série du Gondran près Briançon (Alpes Cottiennes). *Géol. Alp.* **1971**, *47*, 181–201.
40. Dal Piaz, G. Le métamorphisme de haute pression et basse température dans l'évolution structurale du bassin ophiolitique alpino-apenninique (2e partie). *Schweiz. Mineral. Petrol. Mitteilungen* **1974**, *54*, 399–424.
41. Stampfli, G.M.; Borel, G.; Marchant, R.; Mosar, J. Western Alps geological constraints of western Tethyan reconstructions. *J. Virtual Explor.* **2002**, *7*, 75–104. [CrossRef]
42. Rosenbaum, G.; Lister, G. The Western Alps from the Jurassic to Oligocene: Spatio-temporal constraints and evolutionary reconstructions. *Earth-Sci. Rev.* **2005**, *69*, 281–306. [CrossRef]
43. Platt, J.; Behrmann, J.; Cunningham, P.; Dewey, J.; Helman, M.; Parish, M.; Shepley, M.; Wallis, S.; Western, P. Kinematics of the Alpine arc and the motion history of Adria. *Nature* **1989**, *337*, 158–161. [CrossRef]
44. Polino, R.; Dal Piaz, G.; Gosso, G. Tectonic erosion at the Adria margin and acretionary processes for the Cretaceous orogeny in the Alps. In *Deep Structure of the Alps*; Roure, F., Heitzmann, P., Polino, R., Eds.; Société Géologique de France: Paris, France, 1990; Volume 1, pp. 345–367.
45. Stampfli, G.; Marthaler, M. Divergent and convergent margins in the North-Western alps confrontation to actualistic models. *Geodin. Acta* **1990**, *4*, 159–184. [CrossRef]
46. Steck, A.; Hunziker, J. The Tertiary structural and thermal evolution of the Central Alps - compressional and extensional structures in an orogenic belt. *Tectonophysics* **1994**, *238*, 229.254. [CrossRef]
47. Michard, A.; Goffè, B.; Chopin, C.; Henry, C. Did the Western Alps develop through an Oman-type stage? The geotectonic setting of high-pressure metamorphism in two contrasting Tethyan transects. *Eclogae Geol. Helv.* **1996**, *89*, 43–80.
48. Dilek, Y. Collision tectonics of the Mediterranean region: Causes and consequences. *Spec. Pap. Geol. Soc. Am.* **2006**, *409*, 1.
49. Butler, J.; Beaumont, C.; Jamieson, R. The Alps 1: A working geodynamic model for burial and exhumation of (ultra) high-pressure rocks in Alpine-type orogens. *Earth Planet. Sci. Lett.* **2013**, *377*, 114–131. [CrossRef]
50. Ricou, L.; Siddans, W. Collision tectonics in the Western Alps. *Geol. Soc. London, Spec. Publ.* **1986**, *19*, 229–244. [CrossRef]
51. Schmid, S.; Kissling, E.; Diehl, T.; Hinsbergen, D.; Molli, G. Ivrea mantle wedge, arc of the Western Alps, and kinematic evolution of the Alps-Apennines orogenic system. *Swiss J. Geosci.* **2017**, *110*, 581–612. [CrossRef]
52. Tricart, P.; Lemoine, M. The Queyras ophiolite west of Monte Viso (Western Alps): Indicator of a peculiar ocean floor in the Mesozoic Tethys. *J. Geodyn.* **1991**, *13*, 163–181. [CrossRef]
53. Martin, S.; Tartarotti, P.; Dal Piaz, G. Mesozoic ophiolites of the Alps: A review. *Boll. Geofis. Teor. Appl.* **1994**, *36*, 175–219.
54. Tartarotti, P.; Festa, A.; Benciolini, L.; Balestro, G. Record of Jurassic mass transport processes through the orogenic cycle: Understanding chaotic rock units in the high-pressure Zermatt-Saas ophiolite (Western Alps). *Lithosphere* **2017**, *9*, 399–407. [CrossRef]
55. Nicolas, A. Tectonique et métamorphisme dans les Stura di Lanzo (Alpes Occidentales). *Schweiz. Mineral. Petrogr. Mitteilungen* **1969**, *49*, 359–377.
56. Spalla, M.; De Maria, L.; Gosso, G.; Miletto, M.; Pognante, U. Deformazione e metamorfismo della Zona Sesia-Lanzo meridionale al contatto con la Falda Piemontese e con il Massiccio di Lanzo, Alpi Occidentali. *Mem. Della Soc. Geol. Ital.* **1983**, *26*, 499–514.
57. Lagabrielle, Y.; Fudral, S.; Kienast, J. La couverture océanique des ultrabasites de Lanzo (Alpes occidentales): Arguments lithostratigraphiques et pétrologiques. *Geodin. Acta* **1989**, *3*, 43–55. [CrossRef]
58. Cadoppi, P.; Castelletto, M.; Sacchi, R.; Baggio, P.; Carraro, F.; Giraud, V. *Carta Geologica d'Italia alla scala 1:50.000-Foglio 154 Susa e Note illustrative.* Servizio Geologico d'Italia: Roma, Italy, **2002**, 1–123.
59. Balestro, G.; Cadoppi, P.; Perrone, G.; Tallone, S. Tectonic evolution along the Col del Lis-Trana Deformation Zone (internal Western Alps). *Ital. J. Geosci.* **2009**, *128*, 331–339.
60. Gasco, I.; Gattiglio, M.; Borghi, A. Lithostratigraphic setting and P-T metamorphic evolution for the Dora Maira Massif along the Piedmont Zone boundary (middle Susa Valley, NW Alps). *Int. J. Earth Sci.* **2011**. *100*, 1065–1085. [CrossRef]
61. Ghignone, S.; Borghi, A.; Balestro, G.; Castelli, D.; Gattiglio, M.; Groppo, C. HP-tectono-metamorphic evolution of the Internal Piedmont Zone in Susa Valley (Western Alps): New petrologic insight from garnet+chloritoid –bearing micaschists and Fe-Ti metagabbro. *J. Metamorph. Geol.* **2020**. [CrossRef]
62. Sandrone, R.; Leardi, L.; Rossetti, P.; Compagnoni, R. P-T conditions for the eclogitic re-equilibration of the metaophiolites from Val d'Ala di Lanzo (internal Piemontese zone, Western Alps). *J. Metamorph. Geol.* **1986**, *4*, 161–178. [CrossRef]
63. Agard, P.; Monié, P.; Jolivet, L.; Goffé, B. In situ laser probe ^{40}Ar-^{39}Ar dating of the Schistes Lustrés complex: Implications for the exhumation of the Western Alps. *J. Metamorph. Geol.* **2002**, *20*, 599–618. [CrossRef]
64. Lardeaux, J.; Schwartz, S.; Tricart, P.; Paul, A.; Guillot, S.; Béthoux, N.; Masson, F. A crustal-scale cross-section of the south-western Alps combining geophysical and geological imagery. *Terra Nova* **2006**, *18*, 412–422. [CrossRef]
65. Ghignone, S.; Balestro, G.; Gattiglio, M.; Borghi, A. Structural evolution along the Susa Shear Zone: The role of a first-order shear zone in the exhumation of meta-ophiolite units (Western Alps). *Swiss J. Geosci.* **2020**, *133*, 17. [CrossRef]
66. Gasco, I.; Gattiglio, M.; Borghi, A. Review of metamorphic and kinematic data from Internal Crystalline Massifs (Western Alps): PTt paths and exhumation history. *J. Geodyn.* **2013**, *63*, 1–19. [CrossRef]
67. Butler, R.; Freeman, S. Can crustal extension be distinguished from thrusting in the internal parts of mountain belts? A case history of the Entrelor shear zone, Western Alps. *J. Struct. Geol.* **1996**, *18*, 909–923. [CrossRef]

68. Malusà, M.; Polino, R.; Martin, S. The Gran San Bernardo nappe in the Aosta Valley (western Alps): A composite stack of distinct continental crust units. *Bull. Soc. Géolo. Fr.* **2005**, *176*, 417–431. [CrossRef]
69. Festa, A.; Pini, G.; Ogata, K.; Dilek, Y. Diagnostic features and field-criteria in recognition of tectonic, sedimentary and diapiric mélanges in orogenic belts and exhumed subduction-accretion complexes. *Gondwana Res.* **2019**, *74*, 7–30. [CrossRef]
70. Chalot-Prat, F.; Ganne, J.; Lombard, A. No significant element transfer from the oceanic plate to the mantle wedge during subduction and exhumation of the Tethys Ocean (Western Alps). *Lithos* **2003**, *69*, 69–103. [CrossRef]
71. Piccardo, G. Evolution of the lithospheric mantle in an extensional setting: Insights from ophiolitic peridotites. *Lithosphere* **2009**, *1*, 81–87. [CrossRef]
72. Driesner, T. Aspects of petrographical, structural and stable isotope geochemical evolution of ophicarbonate breccias from ocean floor to subduction and uplift; an example from Chatillon, Middle Aosta Valley, Italian Alps. *Schweiz. Mineral. Petrogr. Mitteilungen* **1993**, *73*, 69–84.
73. Lafay, R.; Baumgartner, L.; Schwartz, S.; Picazo, S.; Montes-Hernandez, G.; Vannemann, T. Petrologic and stable isotopic studies of a fossil hydrothermal system in ultramafic environment (Chenaillet ophicalcites, Western Alps, France): Processes of carbonate cementation. *Lithos* **2017**, *294-295*, 319–338. [CrossRef]
74. Decandia, F.; Elter, P. La zona ofiolitifera del Bracco nel settore compreso tra Levanto e la Val Graveglia (Appennino Ligure). *Mem. Della Soc. Geol. Ital.* **1972**, *11*, 503–530.
75. Tricart, P. Tectoniques superposées dans les calcschistes piémontais du Haut-Cristillan (Queyras, Alpes franco-italiennes). *C. R. Acad. Sci.* **1973**, *76*, 705–708.
76. Marroni, M.; Meneghini, F.; Pandolfi, L. Anatomy of the Ligure-Piemontese subduction system: Evidence from Late Cretaceous–middle Eocene convergent margin deposits in the Northern Apennines, Italy. *Int. Geol. Rev.* **2010**, *52*, 1160–1192. [CrossRef]
77. Barbero, E.; Festa, A.; Saccani, E.; Catanzariti, R.; D'Onofrio, R. Redefinition of the Ligurian Units at the Alps-Apennines junction (NW Italy) and their role in the evolution of the Ligurian accretionary wedge: Constraints from mélanges and broken formations. *J. Geol. Soc.* **2020**, *177*, 562–574. [CrossRef]
78. P. Elter.; Trevisan, L. Olistostromes in the tectonic evolution of the Northern Apennines. In *Gravity and Tectonics*; De Jong, K.A., Scholten, R., Eds.; John Willey and Sons: New York, NY, USA, 1973; Volume 1, pp. 175–188.
79. Marroni, M.; Pandolfi, L. Debris flow and slide deposits at the top of the Internal Liguride ophiolitic sequence, Northern Apennines, Italy: A record of frontal tectonic erosion in a fossil accretionary wedge. *Isl. Arc* **2001**, *10*, 9–21. [CrossRef]
80. Meneghini, F.; Pandolfi, L.; Marroni, M. Recycling of heterogeneous material in the subduction factory: Evidence from the sedimentary mélange of the Internal Ligurian Units, Italy. *J. Geol. Soc.* **2020**, *177*, 587–599. [CrossRef]
81. Penrose Conference Participants. Penrose field conference on ophiolites. *Geotimes* **1972**, *17*, 24–25.
82. Dilek, Y.; Furnes, H. Ophiolite genesis and global tectonics: Geochemical and tectonic fingerprinting of ancient oceanic lithosphere. *Geol. Soc. Am. Bull.* **2011**, *123*, 387–411. [CrossRef]